

Brain microvasculature has a common topology with local differences in geometry that match metabolic load

Supplemental Information

Contents

Supplemental Figures.....	2
Figure S1: Labeling and reconstruction quality quantification, related to Figure 1	2
Figure S2: Estimated Point Spread Function (PSF) size in Brain1, related to Figure 2.....	4
Figure S3: Quantify sample deformation, related to Figure 2 and STAR Methods	5
Figure S4: Cumulative density functions of capillary-to-all-vessel ratio in all the 240-cubes within the brains, related to Figure 6.....	6
Figure S5: Sensitivity analysis of windows in local extrema searching, related to STAR Methods	7
Supplemental Tables	8
Table S1: Quantification of the graph refinement classifiers, related to Figure 1.....	8
Table S2: Whole brain wide reconstructed graphs statistics, related to Figure 1 and 2.	9
Table S4: Regional names and abbreviations look-up table, related to Figure 4 and 5.	10
Table S5: Data for generating Figure 7E.	12
Table S6: Additional data for generating Figure 7F.	13

Supplemental Figures

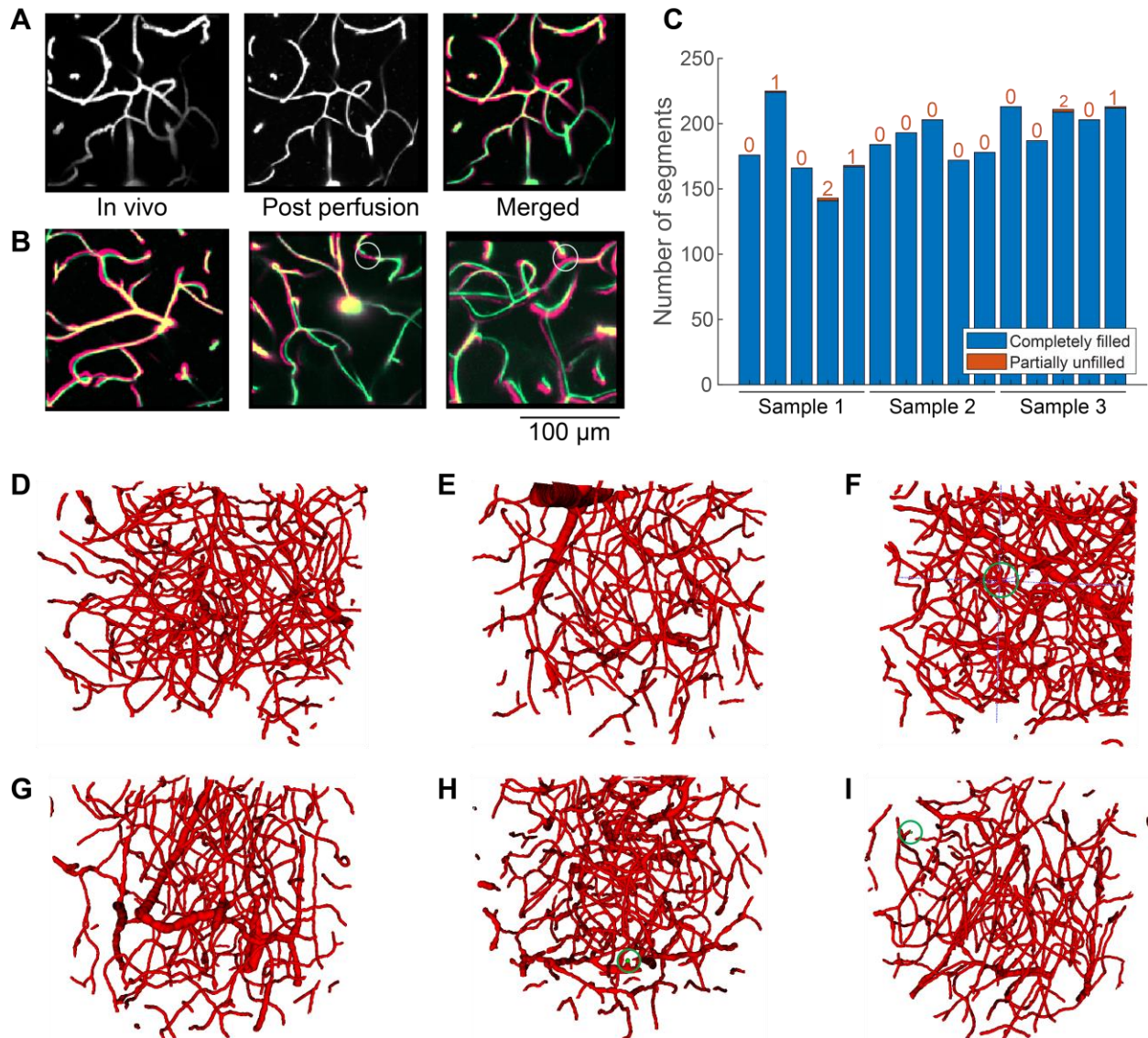


Figure S1: Labeling and reconstruction quality quantification, related to Figure 1

- (A) 60 μ m thick maximum intensity projection of *in vivo* vascular image, registered post perfusion image and their overlay (Red channel: *in vivo*; Green channel: post perfusion; Blue channel: average of *in vivo* and post perfusion image grayscale value; the same as panel **B**). For *in vivo* images, stronger absorption in the pial vessels may shadow the microvessels underneath and lead to uneven signal-to-noise level across the image.
- (B) 60 μ m thick maximum intensity projection of merged *in vivo* and post-perfusion vascular images. The first image shows a complete labeling. The second and third images show two rare examples of partially unfilled vessel segments (circled).
- (C) Cerebral vascular labeling completeness quantification in 15 volumes from 3 brain samples. Each volume is about 180 x 180 x 400 μ m³. 7 out of 2835 vessel segments were found to be partially unfilled.

- (D) The microvascular network is reconstructed as interconnected red curved cylinders in a $240 \times 240 \times 240 \mu\text{m}^3$ volume, the same as panels **E** to **I**. The 240-cube is randomly sampled from the primary somatosensory cortex and has 424 vessel segments and 208 nodes. No connectivity error is founded.
- (E) Reconstruction in ventral auditory cortex with 306 branches, 148 nodes. No connectivity error is founded.
- (F) Reconstruction in thalamus ventral nucleus with 421 branches, 199 nodes. One potential false positive connection between two capillaries is circled and localized by the blue crosshair.
- (G) Reconstruction in pontine reticular nucleus with 279 branches, 199 nodes. No connectivity error is founded.
- (H) Reconstruction in superior colliculus with 381 branches, 186 nodes. One false positive branch with an unconnected endpoint (green) due to perfusion artefact was circled.
- (I) Reconstruction in the secondary motor cortex and anterior cingulate cortex, with 322 branches, 160 nodes. One branch with an unconnected endpoint (green) is circled.

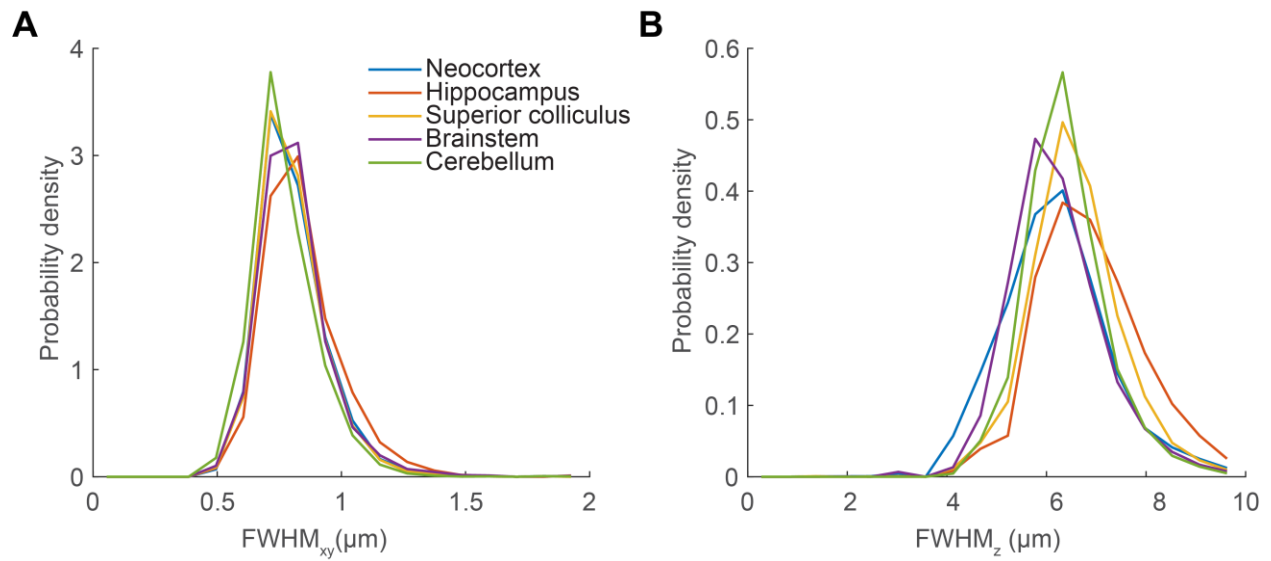


Figure S2: Estimated Point Spread Function (PSF) size in Brain1, related to Figure 2

(A) Lateral full-width-at-half-maximum (FWHM) of the PSF estimated in five brain regions.

(B) Axial FWHM of the PSF in five brain regions. Number of estimations in both panels: neocortex 9,944; hippocampus 2,368; superior colliculus 5,051; brainstem 4,537; cerebellum 5,268.

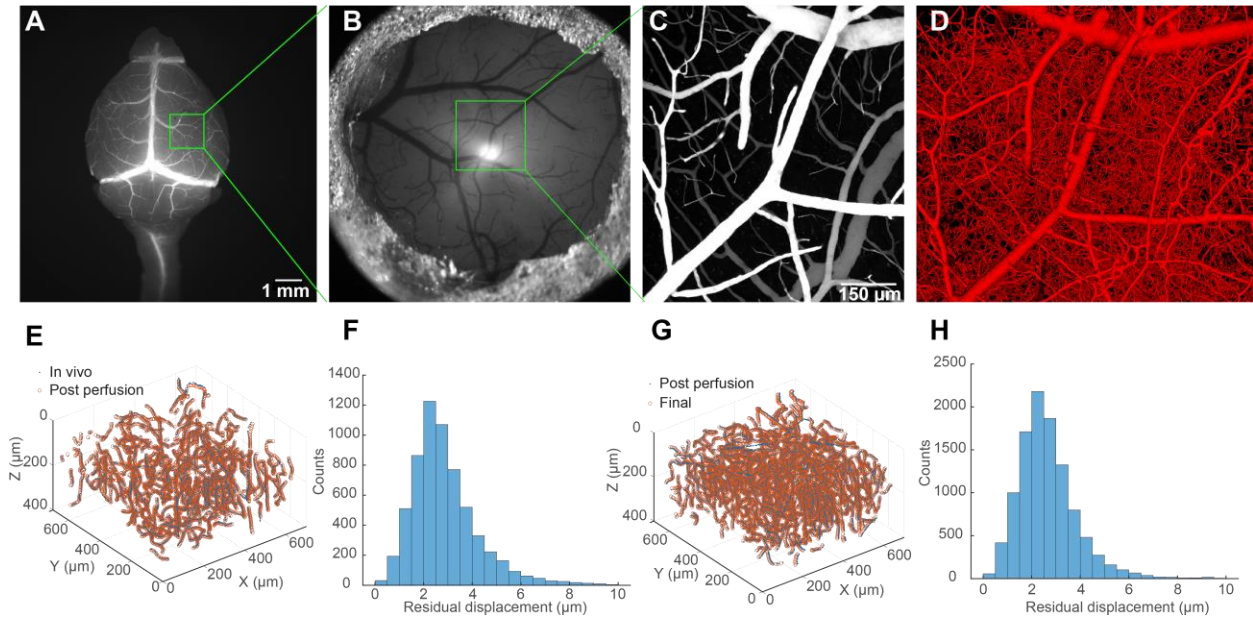


Figure S3: Quantify sample deformation, related to Figure 2 and STAR Methods

- (A) Overview of Brain2 with fluorescent gel-filled vessels.
- (B) Overview of cerebral surface vessels through a cranial window for *in vivo* and post-perfusion imaging.
- (C) Max intensity projection of the surface vessels in *in vivo* image.
- (D) Vessel reconstruction from whole brain imaging.
- (E) Aligning post perfusion vessel reconstruction centerline voxels to the *in vivo* reconstruction (Similarity transformation, scaling factor 1.0003).
- (F) Histogram of residual displacement between 6,227 matched centerline voxel pairs in panel E.
- (G) Aligning whole brain reconstruction vessel centerline voxels to the post perfusion reconstruction (Affine transformation, with linear scaling factors in three directions 1.0490, 1.0534 and 1.0510, respectively).
- (H) Histogram of residual displacement between 10566 matched centerline voxels in panel G.

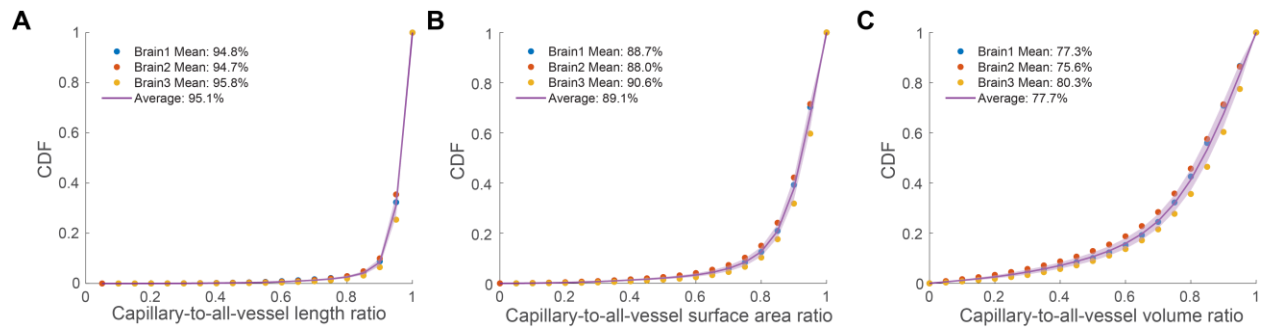


Figure S4: Cumulative density functions of capillary-to-all-vessel ratio in all the 240-cubes within the brains, related to Figure 6

- (A) Ratio between the total capillary length and the total vessel length within the 240-cubes.
- (B) Ratio between the total capillary surface area and the total vessel surface area within the 240-cubes.
- (C) Ratio between the total capillary volume and the total vessel volume within the 240-cubes.

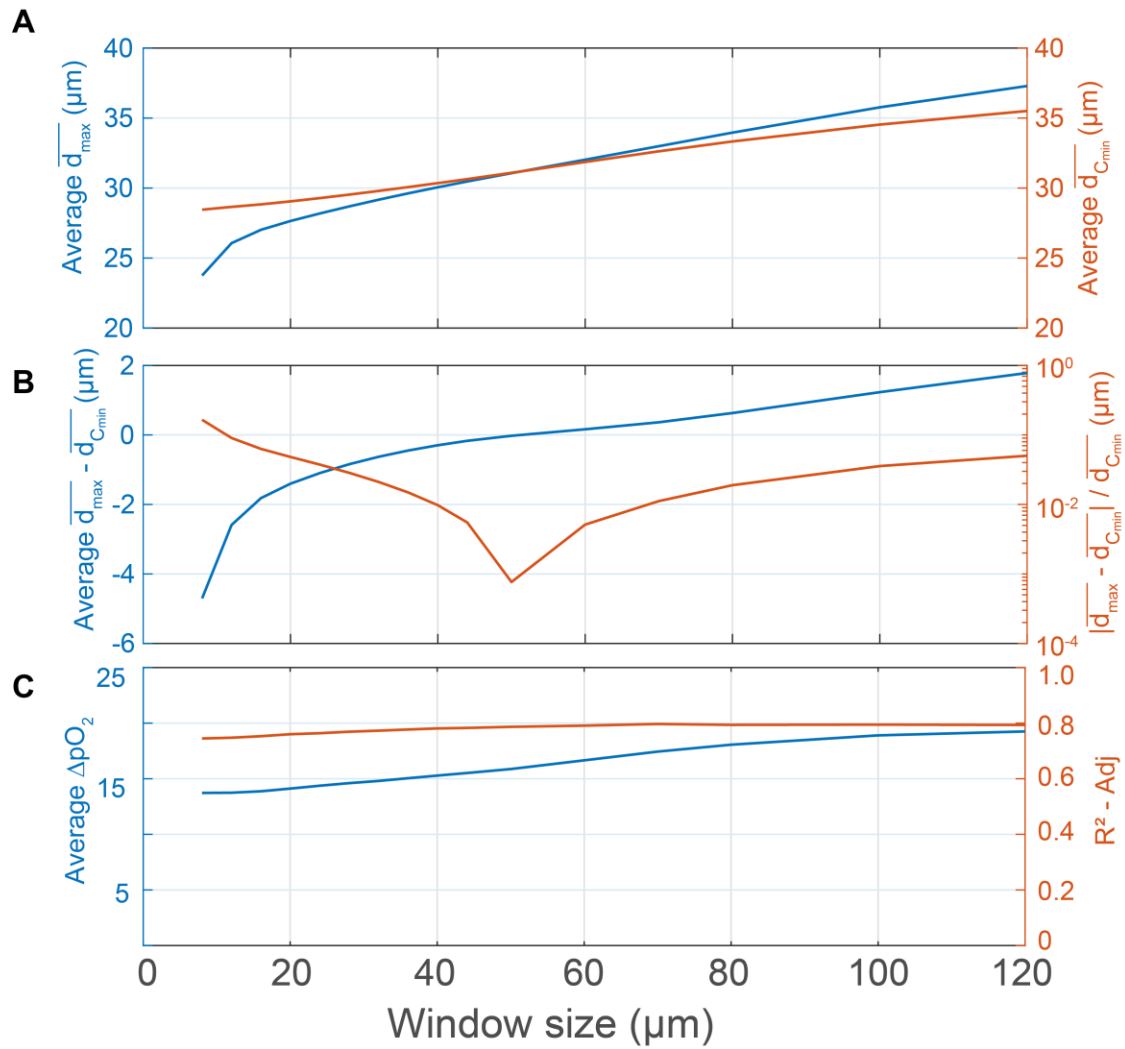


Figure S5: Sensitivity analysis of windows in local extrema searching, related to STAR Methods

- (A) Brain-wide average of $\overline{d_{max}}$ (left) and $\overline{d_{cmin}}$ (right) increase slowly with the window size at different rate and intersect at $w = 50 \mu m$.
- (B) Difference (left) and normalized difference (right) between average $\overline{d_{max}}$ and $\overline{d_{cmin}}$ are minimized at $w = 50 \mu m$.
- (C) Average pO_2 drop ΔpO_2 (left) and the coefficient of determination R^2 (right) increases slowly with window size.

Supplemental Tables

Table S1: Quantification of the graph refinement classifiers, related to Figure 1

Integers under each item are the number of vessel segments (annotated links or linkers) in the test set.

Supplemental Table 1. Classifier performance				
Classifier		Brain1	Brain2	Brain3
Links with one endpoint that need to be deleted	True positive	564	319	70
	True negative	457	194	558
	False positive	19	10	7
	False negative	6	2	6
	Accuracy	97.60%	97.70%	98.00%
Links need to be deleted due to low axial resolution and proximity of vessels	True positive	193	187	217
	True negative	267	150	494
	False positive	5	3	11
	False negative	2	4	7
	Accuracy	98.50%	98.00%	97.50%
Linkers that should not be added	True positive	35	235	28
	True negative	244	405	393
	False positive	2	6	4
	False negative	5	13	3
	Accuracy	97.60%	97.10%	98.40%

Table S2: Whole brain wide reconstructed graphs statistics, related to Figure 1 and 2.

SD is the standard deviation. CV is the coefficient of variation.

Supplemental Table 2. Whole Brain Reconstruction Statistics						
	Brain1	Brain2	Brain3	Average	SD	CV
Brain volume (mm³)	443	434	452	443	9	0.02
Number of skeleton voxels	283710360	264432433	285710552	2.78E+08	1.18E+07	0.04
Total segment length (m)	395	365	392	384	16	0.04
Number of branches, B	6571475	6036661	6352772	6.32E+06	2.69E+05	0.04
Number of nodes, N	4284051	3948612	4165085	4.13E+06	1.70E+05	0.04
B/N	1.534	1.529	1.525	1.529	0.004	0.003
Fraction of branches in the largest graph component	0.995	0.973	0.993	0.987	0.012	0.01
Length density (m/mm³)	0.892	0.842	0.867	0.867	0.025	0.03
Lateral resolution, ω_{xy} (μm)	0.40 \pm 0.02	0.48 \pm 0.02	0.41 \pm 0.02	-	-	-
Axial resolution, ω_z (μm)	3.18 \pm 0.17	3.82 \pm 0.21	2.84 \pm 0.09	-	-	-

Table S4: Regional names and abbreviations look-up table, related to Figure 4 and 5.

Structure names and abbreviations are from the Allen Atlas.

Supplemental Table 4. Visualized regional name and abbreviation	
Abbreviation	Structure name
ACA	Anterior cingulate area
AI	Agranular insular area
AOB	Accessory olfactory bulb
AON	Anterior olfactory nucleus
AUD	Auditory areas
CA	Ammon's horn
CBN	Cerebellar nuclei
CBX	Cerebellar cortex
cc	corpus callosum
COA	Cortical amygdalar area
CTXsp	Cortical subplate
DG	Dentate gyrus
DP	Dorsal peduncular area
ECT	Ectorhinal area
FC	Fasciola cinerea
FRP	Frontal pole cerebral cortex
GU	Gustatory areas
HY	Hypothalamus
IG	Induseum griseum
ILA	Infralimbic area
MBmot	Midbrain motor related
MBsen	Midbrain sensory related
MBsta	Midbrain behavioral state related
MO	Somatomotor areas
MOB	Main olfactory bulb
MY	Medulla
NLOT	Nucleus of the lateral olfactory tract
ORB	Orbital area
P	Pons
PAA	Piriform-amygdalar area
PAL	Pallidum
PERI	Perirhinal area
PIR	Piriform area
PL	Prelimbic area
PTLp	Posterior parietal association areas
RHP	Retrohippocampal region

RSP	Retrosplenial area
SS	Somatosensory areas
STR	Striatum
TEa	Temporal association areas
TH	Thalamus
TR	Postpiriform transition area
TT	Taenia tecta
VIS	Visual areas
VISC	Visceral area

Table S5: Data for generating Figure 7E.

“Number of cubes” are the numbers of 240-cubes included in the regions.

Supplemental Table 5. Plot data for figure 7E																							
Region Name	Glucose metabolism rate (M/s)		Vessel length density (m/mm ³)									Average d _{max} (µm)									Number of cubes		
	Mean	SD	Median			25 percentiles			75 percentiles			Median			25 percentiles			75 percentiles					
			Brain 1	Brain 2	Brain 3	Brain 1	Brain 2	Brain 3	Brain 1	Brain 2	Brain 3	Brain 1	Brain 2	Brain 3	Brain 1	Brain 2	Brain 3	Brain 1	Brain 2	Brain 3	Brain 1	Brain 2	Brain 3
Internal capsule	6.77E-06	6.08E-07	0.65	0.51	0.65	0.58	0.46	0.60	0.69	0.56	0.78	37.4	41.4	36.4	36.4	38.7	32.8	39.0	43.5	38.0	28	31	28
Globus-pallidus	7.47E-06	3.99E-07	0.92	0.77	0.82	0.82	0.68	0.75	1.00	0.84	0.91	30.9	33.8	32.6	29.1	32.0	30.7	33.0	36.2	34.0	67	67	81
Corpus callosum	8.34E-06	5.73E-07	0.55	0.36	0.59	0.50	0.28	0.52	0.63	0.41	0.65	38.8	48.8	38.5	36.3	45.2	35.8	41.5	55.5	40.9	80	134	80
Reticular formation (Mesencephalon)	9.73E-06	4.52E-07	0.95	0.86	0.82	0.87	0.77	0.75	1.06	0.93	0.90	29.3	30.5	30.6	27.5	29.1	29.4	30.6	32.3	32.2	226	225	250
Hippocampus	9.90E-06	4.69E-07	0.72	0.70	0.66	0.65	0.63	0.60	0.80	0.78	0.74	34.2	34.7	35.3	32.2	32.8	33.4	36.3	36.8	37.4	1265	1224	1334
Medial septal nucleus	1.04E-05	8.68E-07	1.01	0.89	0.95	0.91	0.81	0.88	1.09	0.93	0.99	28.3	30.1	29.0	27.1	29.3	28.3	30.1	31.4	30.0	35	37	35
Hypothalamus	1.06E-05	5.38E-07	0.76	0.67	0.72	0.68	0.60	0.65	0.85	0.76	0.82	33.5	35.7	33.9	31.4	33.4	31.8	35.6	37.5	35.7	870	821	925
Lateral septal nucleus	1.06E-05	7.47E-07	0.71	0.59	0.64	0.63	0.48	0.57	0.75	0.64	0.69	34.6	37.9	36.3	33.3	36.0	34.3	36.6	41.9	38.8	169	202	161
Pyramidal cortex	1.06E-05	6.60E-07	0.68	0.70	0.70	0.59	0.62	0.63	0.82	0.83	0.83	34.8	33.8	34.1	31.3	30.8	31.3	37.3	36.4	36.2	399	401	397
Substantia nigra	1.06E-05	5.73E-07	0.85	0.81	0.79	0.78	0.74	0.71	0.93	0.92	0.88	30.8	31.6	31.8	29.4	30.0	30.0	32.6	33.9	33.7	82	76	101
Reticular formation (Brainstem)	1.15E-05	6.08E-07	0.93	0.95	0.89	0.87	0.88	0.82	1.02	1.04	0.99	29.2	29.0	29.6	27.9	27.7	28.0	30.3	30.3	30.8	1409	1280	1491
Insular cortex	1.29E-05	7.29E-07	0.73	0.74	0.77	0.66	0.68	0.71	0.81	0.82	0.85	32.9	32.8	32.1	31.0	30.8	30.6	34.7	34.3	34.0	335	267	314
Red nucleus	1.29E-05	5.21E-07	1.25	1.04	0.97	1.16	0.97	0.87	1.36	1.14	1.06	25.8	27.3	28.2	24.8	26.3	27.3	26.8	28.1	30.0	32	38	41
Caudate nucleus	1.32E-05	5.04E-07	0.91	0.84	0.83	0.84	0.76	0.77	0.97	0.91	0.90	30.2	31.4	31.3	29.0	29.8	30.1	31.7	33.6	32.9	1598	1627	1613
Pons	1.37E-05	5.90E-07	0.97	0.93	0.87	0.86	0.84	0.79	1.14	1.13	1.03	28.9	29.4	30.1	26.6	26.7	27.8	30.5	31.0	31.6	956	828	957
Occipital cortex	1.44E-05	4.86E-07	0.86	0.84	0.87	0.78	0.77	0.79	0.93	0.92	0.93	30.0	30.2	29.9	28.7	28.7	28.6	31.8	32.0	31.8	682	609	642
Lateral geniculate (Thalamus)	1.48E-05	5.38E-07	1.19	1.15	1.04	1.10	0.95	1.00	1.27	1.22	1.12	26.1	26.8	27.3	25.1	25.2	26.1	27.2	29.0	28.2	34	29	39
Ventral nucleus (Thalamus)	1.51E-05	6.95E-07	1.18	1.03	1.00	1.11	0.96	0.95	1.26	1.13	1.07	26.5	28.0	28.1	25.3	26.4	27.0	27.5	29.3	28.9	216	228	266
Superior colliculus	1.58E-05	4.86E-07	1.01	0.91	0.93	0.95	0.85	0.86	1.12	1.00	1.00	28.1	29.3	29.1	26.6	27.8	28.1	29.1	30.5	30.3	454	417	500
Cingulate gyrus	1.60E-05	5.56E-07	0.92	0.86	0.89	0.86	0.80	0.82	0.97	0.95	0.95	29.2	30.3	29.8	28.3	28.8	28.8	30.3	32.0	31.1	250	277	239
Medial geniculate (Thalamus)	1.62E-05	7.64E-07	1.13	1.09	1.00	1.02	0.95	0.92	1.23	1.17	1.09	26.7	27.0	27.6	25.4	25.7	26.3	28.7	28.7	29.1	17	22	25
Parietal cortex	1.62E-05	5.04E-07	1.04	1.02	1.02	0.93	0.88	0.91	1.14	1.13	1.12	27.2	27.3	27.5	26.0	25.9	26.2	28.9	29.4	29.2	1908	2003	1881
Anterior nucleus (Thalamus)	1.70E-05	5.04E-07	1.28	1.13	1.09	1.20	1.03	1.03	1.38	1.20	1.17	25.1	26.7	27.1	24.0	25.8	26.0	28.5	28.0	93	110	134	
Cochlear nucleus	1.74E-05	8.51E-07	1.56	1.53	1.58	1.46	1.38	1.39	1.65	1.73	1.73	22.6	22.5	22.5	22.0	20.8	21.0	23.4	24.3	23.5	35	31	40
Superior olive	1.81E-05	7.12E-07	1.45	1.48	1.40	1.18	1.32	1.28	1.61	1.58	1.53	23.3	22.9	23.6	22.3	22.4	22.3	25.8	24.4	24.3	23	30	30
Vestibular nucleus	1.88E-05	6.08E-07	1.44	1.45	1.35	1.29	1.30	1.22	1.57	1.58	1.44	23.4	23.5	24.0	22.5	22.3	23.0	24.8	24.8	25.3	165	125	168
Inferior colliculus	2.22E-05	7.29E-07	1.50	1.49	1.45	1.27	1.28	1.29	1.75	1.70	1.57	22.4	22.7	22.8	20.7	21.0	21.8	24.7	24.1	24.3	183	173	195

Table S6: Additional data for generating Figure 7F.

Oxygen metabolism rates are averages over references. Radii are capillary radius from the references.

Supplemental Table 6 Extra plot data for Figure 7F							
Species	Region	Length density (m/mm ³)	Density reference	k_{O_2} ($\frac{\mu mol}{100 g \cdot min}$)	Metabolism references	Radius (μm)	Radius reference
Macaque	Visual cortex	0.478	Weber et al., 2008	325	Kennedy et al., 1978	2.75	Weber et al., 2008
Human	Primary motor cortex	0.499	Cassot et al., 2006	185	Vafaee et al., 2012	3	Cassot et al., 2006
Human	Frontal cortex	0.363	Fernandez-Klett et al., 2020	181	Ishii et al., 1996; Karbowski, 2014; Kuhl et al., 1982; Pantano et al., 1984	3	Cassot et al., 2006
Human	Thalamus	0.281	Kubikova et al., 2018	183	Pantano et al., 1984; Kuhl et al., 1982; Heiss et al., 1984; Hatazawa et al., 1995	3	Cassot et al., 2006
Human	Pons	0.291	Kubikova et al., 2018	120	Heiss et al., 1984; Hatazawa et al., 1995	3	Cassot et al., 2006
Human	White matter	0.160	Kubikova et al., 2018	90	Pantano et al., 1984; Heiss et al., 1984; Hatazawa et al., 1995	3	Cassot et al., 2006
Human	Cerebellum cortex	0.296	Kubikova et al., 2018	179	Tomasi et al., 2013; Heiss et al., 1984; Hatazawa et al., 1995	3	Cassot et al., 2006
Human	Caudateputamen	0.347	Kubikova et al., 2018	210	Kuhl et al., 1982; Heiss et al., 1984; Hatazawa et al., 1995	3	Cassot et al., 2006
				Average over all references			